Journal of Structural Geology 173 (2023) 104910

Contents lists available at ScienceDirect

Journal of Structural Geology

journal homepage: www.elsevier.com/locate/jsg

Quantitative analyses of deformation band occurrence and host rock properties in pyroclastic rocks of eastern Taiwan

Chih-Cheng Chung [a,b], Chih-Tung Chen [a,*], Chia-Yu Lu [c]

[a] Department of Earth Sciences, National Central University, Zhongli, Taiwan
[b] Institute of Nuclear Energy Research, Atomic Energy Council, Executive Yuan, Longtan, Taiwan
[c] Department of Geosciences, National Taiwan University, Taipei, Taiwan

ARTICLE INFO

Keywords:
Deformation bands
Lithological effect
Pyroclastic rocks
Convergent plate boundary
Taiwan arc-continent collision

ABSTRACT

We analyze deformation bands found in a pyroclastics locality at the Shitiping outcrop in eastern Taiwan, allowing close inspection of their features and evolution. To quantify their occurrences and strain distribution, we characterize the architecture of deformation bands based on detailed field investigation, including deformation band frequency, core thickness, cluster width, core displacement, and cluster displacement. We observe that the attitude, deformation style, quantitative characteristics, and microstructure of the deformation bands at the Shitiping outcrop correlate with the porosity, grain size, sorting coefficient, and the derived mean grain crushing pressure which are calculated from grain size and porosity of their host pyroclastic rocks. The frequency of deformation bands is positively correlated to the porosity and inversely proportional to average grain size and sorting coefficient of host pyroclastic layers, indicating that deformation is more localized in coarse-grained pyroclastic rocks. The band frequency is negatively correlated to the deformation band maximum displacement, core thickness, and cluster width; and maximum core thickness is negatively correlated to mean grain crushing pressure. Conversely, maximum core thickness of deformation band is positively correlated to sorting coefficient and average grain size of host rock, suggesting that the maximum core thickness might be affected by maximum grain size of pyroclastic layers. Our results indicate that the host rock properties contribute in affecting the occurrences of deformation bands.

1. Introduction

In response to applied stress, the structures and deformation mechanisms that occur in high porosity materials differ from those in continuum materials. For example, porous materials tend to form deformation bands rather than joints or fractures (Fossen et al., 2007, 2018). Deformation bands are commonly tabular strain localization structures occurring in a variety of porous rocks such as sandstones, pyroclastic rocks and carbonate rocks with porosity exceeding 15%. The patterns of deformation bands inform mechanisms of deformation (Cashman and Cashman, 2000; Fossen et al., 2007; Rotevatn et al., 2008, 2016; Wilson et al., 2003), including how stress and strain were distributed under various tectonic regimes (Ballas et al., 2014; Davatzes et al., 2003; Fossen et al., 2018; Schultz and Siddharthan, 2005; Soliva et al., 2016). Unlike brittle fractures, deformation bands tend to reduce porosity and permeability of the host rock and increase cohesion (Antonellini et al., 1994; Ballas et al., 2015; Fossen et al., 2007; Kaproth et al., 2010), with implications for subsurface hydrocarbon migration and carbon dioxide storage (Antonellini and Aydin, 1994; Fossen et al., 2007; Hesthammer and Fossen, 2000; Shipton et al., 2005). The effects on fluid flow path depend on the frequency and permeability of the deformation bands (Rotevatn et al., 2009), which are influenced by the tectonic regime and lithological properties (Ballas et al., 2014; Cheung et al., 2012; Fossen et al., 2007; Rotevatn et al., 2016; Rustichelli et al., 2012; Schultz et al., 2010; Soliva et al., 2016; Soliva et al., 2013). Quantitative documentation of the properties of deformation bands and host rocks is thus crucial for scientific and engineering purposes. While deformation bands have been extensively investigated in quartz-rich sandstones, less is known about deformation bands in pyroclastic rocks. Structural analysis of the Reykjanes Peninsula, Iceland reveals that local tectonic controls such as perturbed stress fields and spreading angle obliquity influence fracture pattern and density in pyroclastic rocks (Clifton and Kattenhorn, 2006). Observation of deformation bands in ignimbrites indicates that high-porosity non-welded units deform by

* Corresponding author.
E-mail addresses: kthomasch@gmail.com, chihtung@ncu.edu.tw (C.-T. Chen).

https://doi.org/10.1016/j.jsg.2023.104910
Received 3 September 2022; Received in revised form 14 June 2023; Accepted 21 June 2023
Available online 27 June 2023

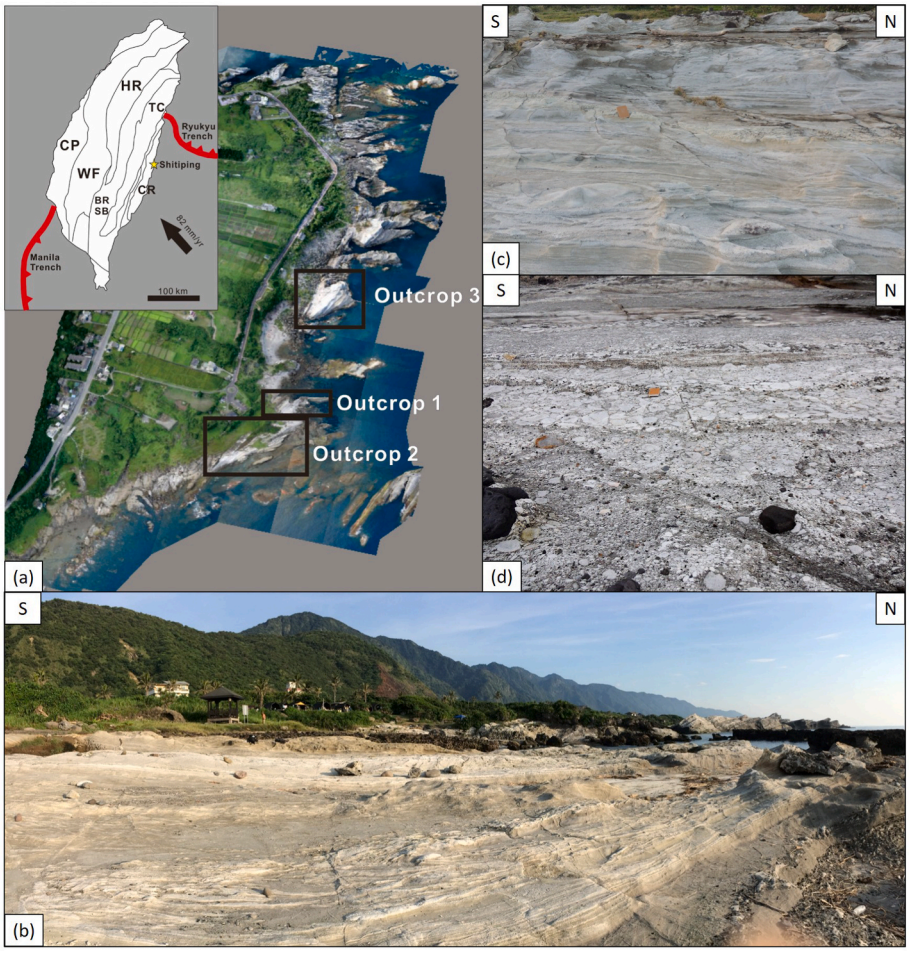

Fig. 1. UAV images of study area and structural cross section. (a) Overview of Shitiping area. Our study focuses on Outcrops 1, 2 and 3. (b) Field photo of outcrop 1. (c) Field photo of outcrop 2. (d) Field photo of outcrop 3.

cataclasis in deformation bands while low-porosity units deform by transgranular fractures (Wilson et al., 2003). The type of fault zone structure is also found affected by the degree of welding (Wilson et al., 2003; Riley et al., 2010). The diagenetic minerals in deformation bands further suggest preferential fluid flow within deformation bands in the vadose zone (Wilson et al. 2003, 2006). However, information on quantitative analysis of deformation bands formed under a strike-slip regime and the impact from lithology are still lacking. This leads to limited knowledge on how contrasting material properties including porosity, grain size, grain shape, and sorting coefficient of pyroclastic rocks affect the distribution and geometry of deformation bands.

The well-developed deformation bands exposed in ignimbrites and tuff-pyroclastics at the Shitiping locality of the Coastal Range, eastern Taiwan (Cavailhes and Rotevatn, 2018) offer a valuable opportunity to characterize deformation bands in pyroclastic rocks, and then quantitatively assess the impact of lithological properties on deformation band development. The island arc origin of the Shitiping pyroclastics, which are now part of the collided arc (Lu and Hsu, 1992; Teng, 1990), also suggests that the deformation bands may reflect the rheology of onshore to near-shore eruptive volcanics that emerges during the transition in tectonic environment from overriding plate at a subduction zone to within a collisional orogenic belt.

This study aims to quantitatively document and explore how lithological properties influence deformation band occurrence through new analysis of pyroclastic rocks at the Shitiping locality. We investigate how host rock characteristics affect the development of deformation bands and consequently deformation pattern, with the goal of understanding strain distribution and rheology of pyroclastic rocks. We focus on: (1) defining and documenting the characteristics of deformation band occurrence including displacement, core thickness, cluster width, and frequency; (2) determining host rock properties including porosity, grain size, sorting coefficient and the derived mean grain crushing pressure; and (3) investigating the relationship between intrinsic host-rock properties and the characteristics of deformation band occurrence; and (4) discussing the implications for lithological effects on deformation band development.

2. Geological background

To address the question on how occurrences of deformation bands are influenced by rock properties, we focus on the site of Shitiping, located in the Coastal Range of eastern Taiwan. The Coastal Range, which is dominated by series of volcanic rocks, is the remnant of the northern part of the Luzon Arc that resulted from South China Sea subduction and the following and ongoing arc-continent collision (Lu and Hsu, 1992; Teng, 1990). The Shitiping outcrop comprises poorly-sorted subaerial to tidal deposited ignimbrites and pyroclastic rocks, the product of explosive eruptions before 4.2 Ma based on $^{40}Ar/^{39}Ar$ dating and zircon U–Pb ages (Huang et al., 1988; Lai et al., 2017).

The ignimbrites, commonly with welded structures, are matrix-supported and predominantly composed of vesicular glassy shards and pumices with minor amounts of lithic fragments. Most of the glassy shards and pumice fragments are rounded, whereas lithic fragments are angular (Song, 1990; Song and Lo, 1987, 2002). Tuff layers exposed at Shitiping are usually porous coarse tuffs with grain sizes larger than

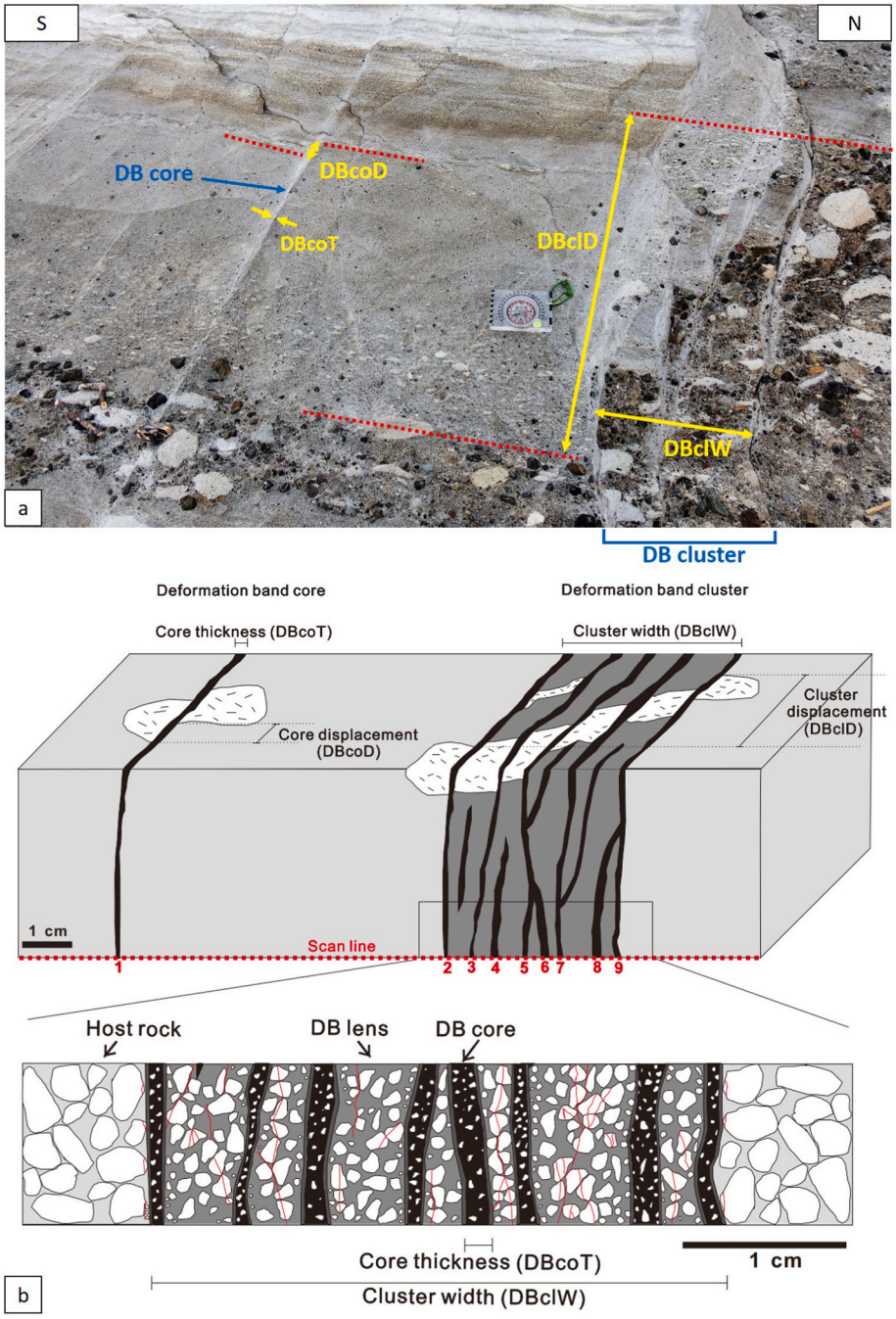

Fig. 2. (a) Field photo demonstrating measurements of deformation band core thickness (DBcoT), deformation band core displacement (DBcoD), deformation band cluster width (DBclW) and deformation band cluster displacement (DBclD). (b) Architecture of deformation bands in pyroclastic rocks and illustrated definition of key deformation band parameters: deformation band core thickness (DBcoT), deformation band cluster width (DBclW), and deformation band core and cluster displacement (DBcoD, DBclD). Deformation band core thickness describes how thick a single band core is, which is defined as the distance between the two boundaries of grain size and porosity reduction of the deformation band core. Cluster width describes how wide a band cluster is and is defined by the distance between the outermost deformation band cores of an individual deformation band cluster. Displacement of deformation band cluster and core is also illustrated.

0.25 mm (Gillespie and Styles, 1999) and porosity exceeding 16% (Lin and Huang, 2017). These tuffs contain 55–80% crystal grains, including plagioclase, amphibolite, pyroxene, germarite, and magnetite (Song, 1990; Song and Lo, 1987, 2002), and 20–45% glassy and lithic fragments.

The Shitiping study site is a ~200 m wide and ~1500 m long area that contains three outcrops located along the east limb of the Shitiping Syncline (Fig. 1). The deformation bands are widely distributed in the Shitiping outcrops, and generally appear as erosion-resistant multi-strand clusters with meter-scale length and 0.1–15 cm width. The appearances of deformation bands are usually band cluster in which deformation bands entangle with each other, or single strand of deformation bands (Lin and Huang, 2017). They were initially documented as micro-faults by Lai (1995) and more recently as deformation bands by Lin and Huang (2017). Cavailhes and Rotevatn (2018) classified these deformation bands into three types: disaggregation-dominated pure compaction bands (PCB), cataclastic flow-dominated reverse-sense compactional shear bands (RCSB), and transverse-sense compactional shear bands (TCSB). The porosity of RCSBs and TCSBs are 3–7%, while the porosity of PCBs is 17–22% (Cavailhes and Rotevatn, 2018), indicating strong shear-enhanced compaction in the deformation bands. Unlike TCSBs, PCBs and RCSBs only occur in host rocks with certain grain size and porosity ranges, suggesting that rock mechanical properties influence the development of deformation bands at Shitiping.

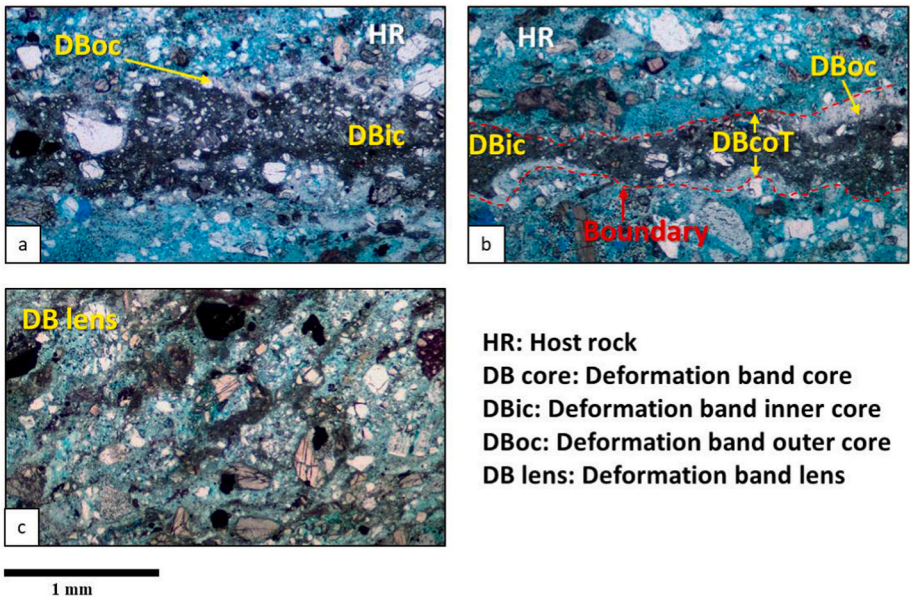

Fig. 3. Photomicrographs of deformation band core, deformation band lens and host rock. (a) Matrix-supported deformation band core showing grain size and porosity reduction, with sharp boundaries between host rock and band core, and between highly deformed inner core and less deformed outer core. (b) Irregular and sharp boundaries between host rock and band core, and between highly deformed inner core and less deformed outer core. The thickness of inner core and outer core vary along strike of the deformation band. (c) Deformation band lenses characterized by intra- and inter-granular fractures, indicating presence of strain.

3. Methodology - fabric characterization of deformation bands and field/microscopic data acquisition

3.1. Deformation band core thickness (DBcoT)

Deformation band core in our study is a strand of deformation band whether it entangles with another DB core, which means that a DB core can be observed as single strand or in a DB cluster (Fig. 2). Our criteria for identifying the deformation band core of Type 3 deformation bands are shown in Figs. 2 and 3, and include.

(i) Compared with pyroclastic host rocks, deformation band cores show obvious porosity reduction, grain fracturing, cataclasis and mineral alteration that can be observed in the field or under microscope (Fig. 3).

(ii) For deformation bands forming a zone with intervening less-deformed deformation band lenses, we identify deformation band cores from thin tabular structures with obvious porosity reduction, grain fracturing and alteration phenomena, where the original texture of host rock is totally obliterated and cannot be observed.

Because the damage zones of deformation band cores are not obvious in the field and usually less than 0.5 mm in thickness (Fig. 3), we exclude the damage zones in our assessment and define the deformation band core thickness (DBcoT) as the distance between the boundaries of deformation band core (Figs. 2 and 3). In cases where the deformation

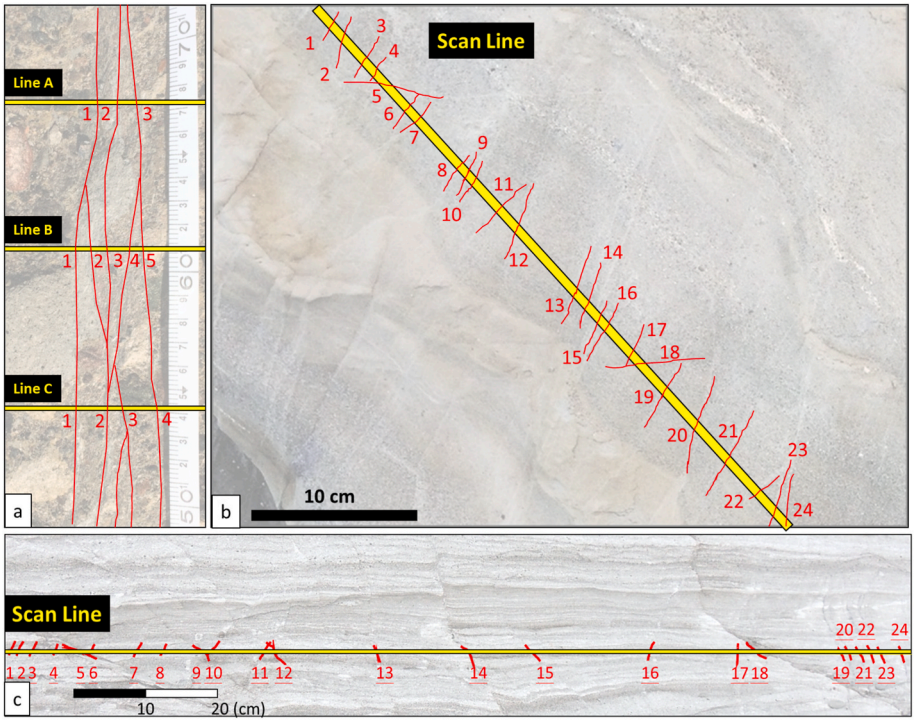

Fig. 4. Field photos and corresponding sketches demonstrating measurement of deformation band frequency. (a, b) The deformation band frequency is measured based on the number of intersections of survey line and deformation band cores. (c, d) The deformation band cluster consists of multiple entangled deformation band cores. These deformation band cores sometimes coalesce or bifurcate in a cluster and influence the number of intersections of survey line and deformation band cores. Thus, the location of survey line may affect the result of deformation band frequency.

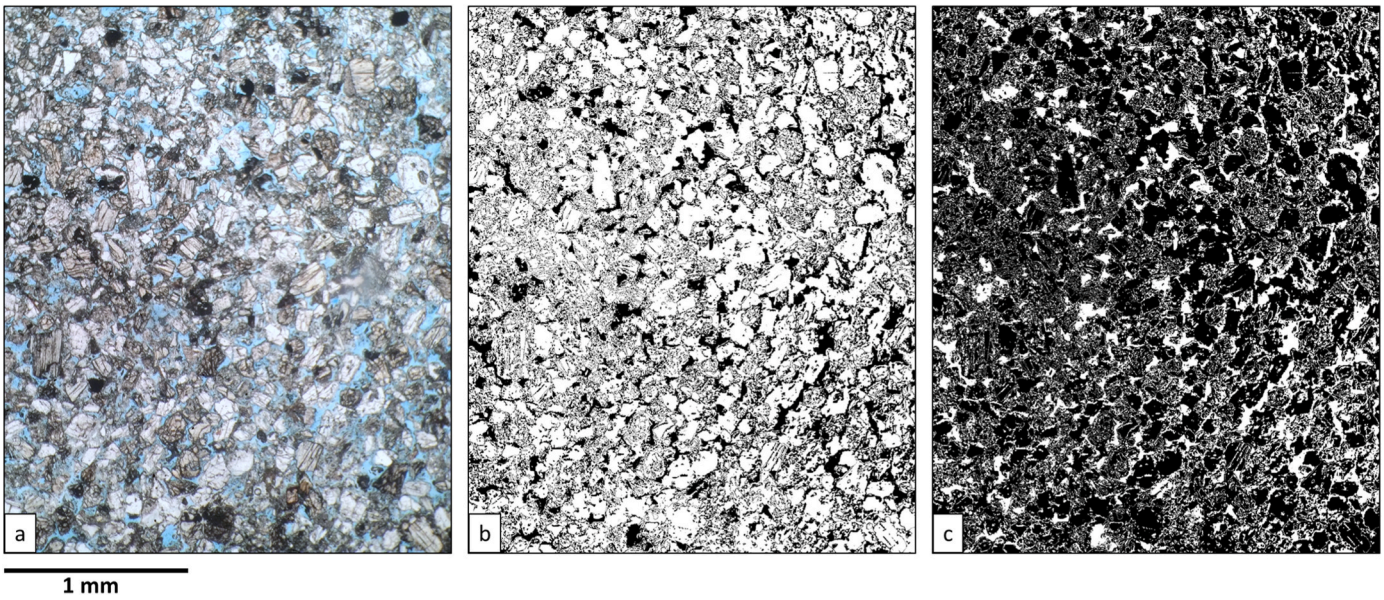

Fig. 5. Examples of porosity analysis and grain size analysis. Pores are picked from the (a) photomicrograph and (b) transformed into a binary image with black pores and white grains for calculating the spatial percentage of pore space. (c) Grains are transformed into black areas, and the grains with clear boundary are picked to do grain size analysis.

band core is characterized by an intensively deformed, matrix supported inner core and less deformed outer core under microscope, the DBcoT is defined by the boundary of outer core (Figs. 2 and 3b). Because of the typically sharp boundaries of the deformation band core, the DBcoT can be measured in the field scale (Fig. 2). The measurements of DBcoT are made perpendicular to the strike of deformation bands.

3.2. Deformation band cluster width (DBclW)

Deformation band cluster mentioned in our study is a narrow zone that deformation band cores are intertwined with each other (Fig. 2). This cluster includes the multi-strand bands described by Ballas et al. (2012). We define deformation band clusters using the following criteria in the field.

(i) Deformation band clusters consist of several deformation band cores with similar attitude, and the intervening deformation band lenses are bounded by these cores. The boundaries of a deformation band cluster are defined by the outermost cores.
(ii) The volumes of rocks trapped within deformation band cluster, which we term deformation band lenses, generally exhibit evidence of deformation that can be observed in the field.
(iii) Deformation band clusters contain obvious deformation and shear displacement up to at least mm scale that can be observed in the field.

Unlike the total band thickness which neglects inter-band distance employed by Philit et al. (2018), we define the deformation band cluster width (DBclW) as the distance between the outermost deformation band cores of an individual deformation band cluster to document to volumetric scale of a deformation band cluster (Fig. 2). In some cases, the damage zone of deformation band cluster can be observed in the field. The boundary between the outermost deformation band core of the cluster and damage zone is typically sharp and can be identified in the field. However, the exact boundaries of damage zone and host rock are usually not observable in the field. Thus, similar to the DBcoT, our measurement of DBclW excludes the damage zone of the deformation band cluster.

3.3. Deformation band core and cluster displacement (DBcoD, DBclD)

For documenting the amount of shear displacement on the deformation band structures, we define the deformation band core displacement (DBcoD) for single bands and the deformation band cluster displacement (DBclD) for deformation band clusters (Fig. 2).

3.4. Deformation band frequency

The attitudes of deformation bands generally strike toward NE-SW or NW-SE. To measure the frequency of deformation bands, we set up scan lines parallel to strike of bedding (209/18 W) and counted the number of deformation bands intersecting the scan lines (Fig. 4). In calculating deformation band frequency, we only consider the number of encountered deformation band cores along the scan line, regardless of their attitude. Unlike the term “band density”, which is the “total band thickness” divided by the “cluster thickness”, introduced by Philit et al. (2018), the deformation band frequency is the number of deformation bands per meter and represents the amount of deformation bands in the field.

3.5. Porosity and grain size analysis

We measured the porosity and average grain size of pyroclastic rocks at Shitiping using image analysis of thin sections orthogonal to the strike of deformation bands. The porosity is defined by the aerial percentage of pore space observed under optical microscope, and the average grain size is measured in 2 dimensions and then transformed into 3 dimensions based on the equation of Kong et al. (2005). To analyze the porosity in thin sections, the pores were dyed with Methylene blue and then transformed into binary images showing pore areas and rock areas in black and white. The porosity was evaluated by calculating the percentages of black pixels in images (Fig. 5). Average grain size was analyzed with similar image processing procedure by manual picking of grains and lithic fragments in the thin section images (Fig. 5). The sorting coefficient was calculated using logarithmic graphical measurement following Folk and Ward (1957). Sorting coefficients higher than 1 indicate poorly-sorted host rocks. Due to the spatial scale of our analyses that are based on optical thin sections, the calculation of average grain size and sorting coefficient excludes the much larger

Table 1
Data of deformation band frequency and lithological characters of rock units.

Outcrop 1	Avg. grain size (mm)	Sorting coefficient	Porosity (%)	Mean grain crushing pressure (MPa)	Band frequency (number/meter)	Maximum cluster displacement (mm)	Maximum core thickness (mm)	Maximum cluster width (mm)
Unit 1	0.44	2.11	7.18	121.09	1.20	400	20	150
Unit 2	0.25	2.91	10.44	168.69	5.83	1100	60	90
Unit 3	0.36	2.88	9.41	111.06	3.86	1150	60	80
Unit 4	0.27	1.27	1.24	3577.85(X)	4.57	1200	10	480
Unit 5	0.22	2.28	16.5	96.95	5.98	1200	10	460
Unit 6	0.28	1.71	8.54	186.56	3.50	1300	5	290
Unit 7	0.26	1.61	11.41	134.56	17.33	190	3	3
Unit 8	0.33	1.53	7.95	166.25	6.43	120	10	30
Unit 9	0.20	1.53	18.53	97.70	13.75	20	3	15
Unit 10	0.30	3.20	9.89	138.68	2.43	X	X	X
Unit 11	0.37	1.20	5.31	253.34	4.43	X	X	X
Unit 13	0.39	2.71	11.67	72.85	2.60	X	X	X
Unit 14	0.36	1.57	1.58	1591.35(X)	1.00	X	X	X
Unit 15	0.16	1.91	7.27	544.33	17.78	X	X	X
Outcrop 2	Avg. grain size (mm)	Sorting coefficient	Porosity (%)	Mean grain crushing pressure (MPa)	Band frequency (number/meter)	Maximum cluster displacement (mm)	Maximum core thickness (mm)	Maximum cluster width (mm)
Unit 1	0.28	1.53	15.33	139.29	1.67	X	X	X
Unit 2	0.25	2.91	10.44	168.69	3.43	1100	60	90
Unit 3	0.18	1.35	5.31	518.53	4.33	X	X	X
Unit 5	0.23	2.28	16.50	96.95	4.13	1200	10	460
Unit 6	0.28	1.71	8.54	186.56	2.13	1300	5	290
Outcrop 3	Avg. grain size (mm)	Sorting coefficient	Porosity (%)	Mean grain crushing pressure (MPa)	Band frequency (number/meter)	Maximum cluster displacement (mm)	Maximum core thickness (mm)	Maximum cluster width (mm)
Unit 1	0.35	1.05	3.94	434.75	2.63	X	X	X
Unit 2	0.36	1.68	9.21	114.70	1.25	X	X	X
Unit 3	0.52	0.61	5.46	145.61	4.00	X	X	X
Unit 4	0.45	1.23	10.29	70.86	1.50	X	X	X
Unit 8 tuff	0.38	1.58	15.62	47.33	3.75	X	X	X
Unit 8 welded tuff	0.28	2.63	8.64	189.49	1.50	X	X	X

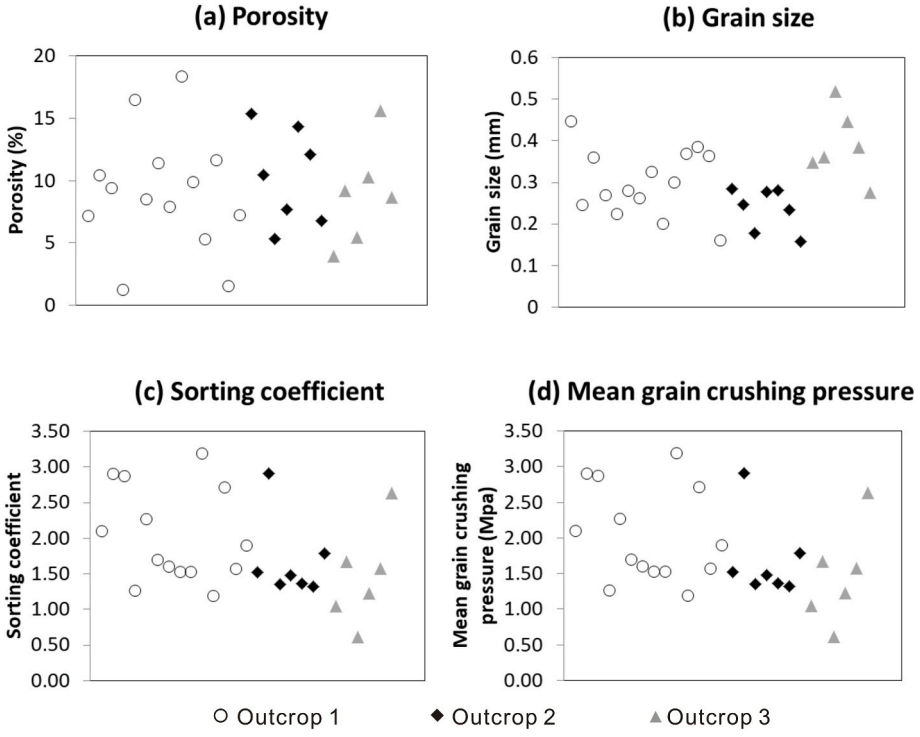

Fig. 6. Plots of (a) porosity, (b) grain size, (c) sorting coefficient and (d) mean grain crushing pressure of host rocks.

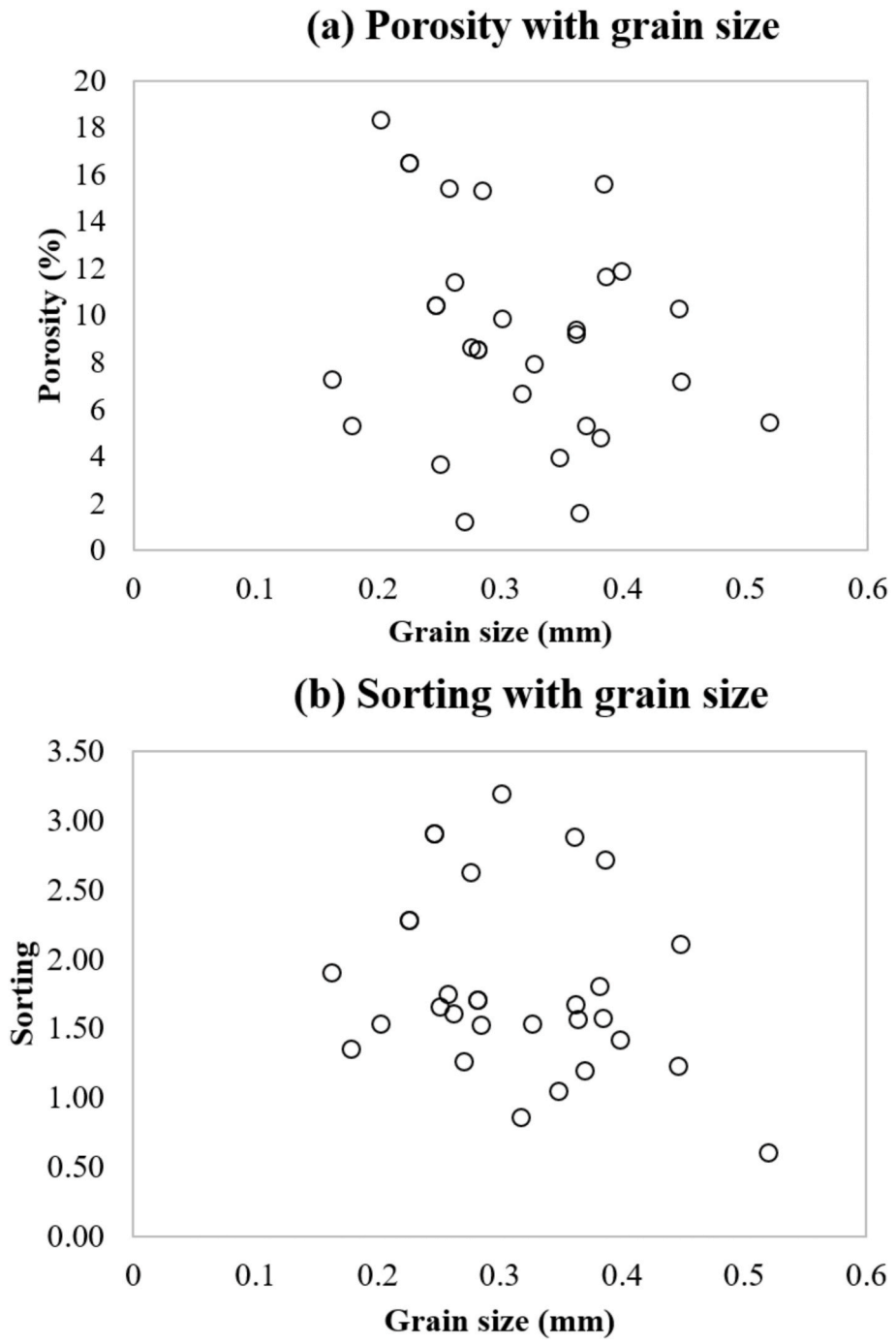

Fig. 7. Plots of (a) porosity with grain size and (b) sorting with grain size. The plots provide evidence that the parameters are independent, while also revealing a significant variation in the characteristics of lithological units.

volcanic bombs, lapilli and pumice (i.e., only matrix material were analyzed).

3.6. Mean grain crushing pressure

Another key host rock characteristic is the mean grain crushing pressure, a measure of the critical pressure for grain crushing under hydrostatic stress regime (Zhang et al., 1990), which is an estimate of the minimum pressure/depth for the formation of the deformation bands. Based on the experimental results of Zhang et al. (1990), the mean grain crushing pressure, P*, is determined using the empirical equation $P^* = (\psi R)^{-1.5}$, where ψ is porosity fraction, R is average grain size in mm, and P* is the mean grain crushing pressure in MPa. We calculated P* using the values of porosity and mean grain size determined by microscopic analysis as described above.

4. Characteristics of host rock and deformation bands at the shitiping locality

4.1. Host rock

The host rocks exposed at the field locality contain a sequence of decimeter-to meter-scale tuffs, ignimbrites, and pyroclastic breccias with different characteristics. These tuffs and ignimbrites are composed

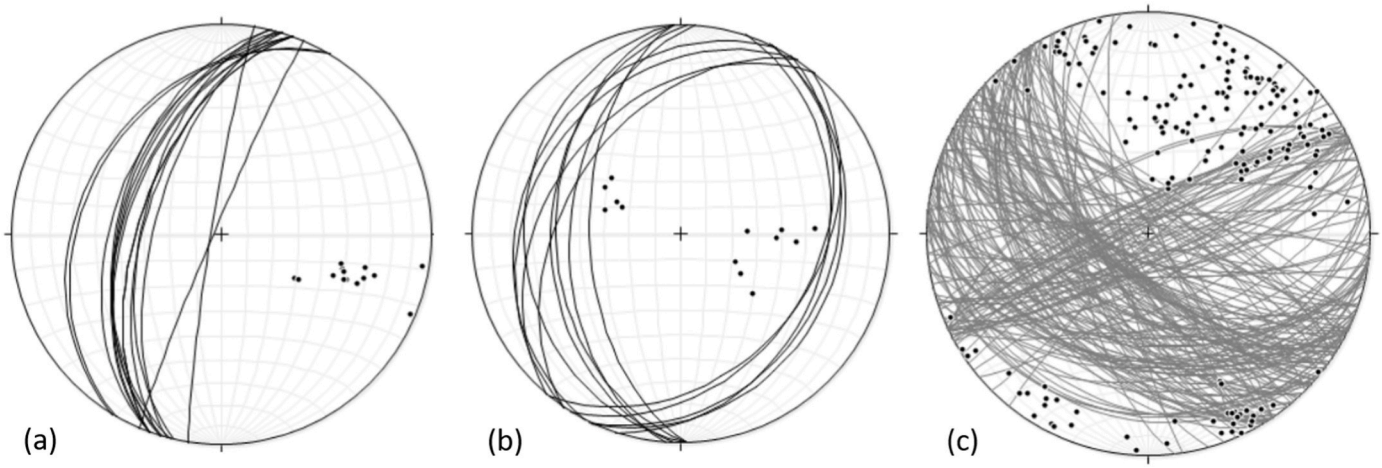

Fig. 8. Equal-area lower hemisphere projection of deformation bands. (a)Type 1 band. (b) Type 2 band. (c) Type 3 band.

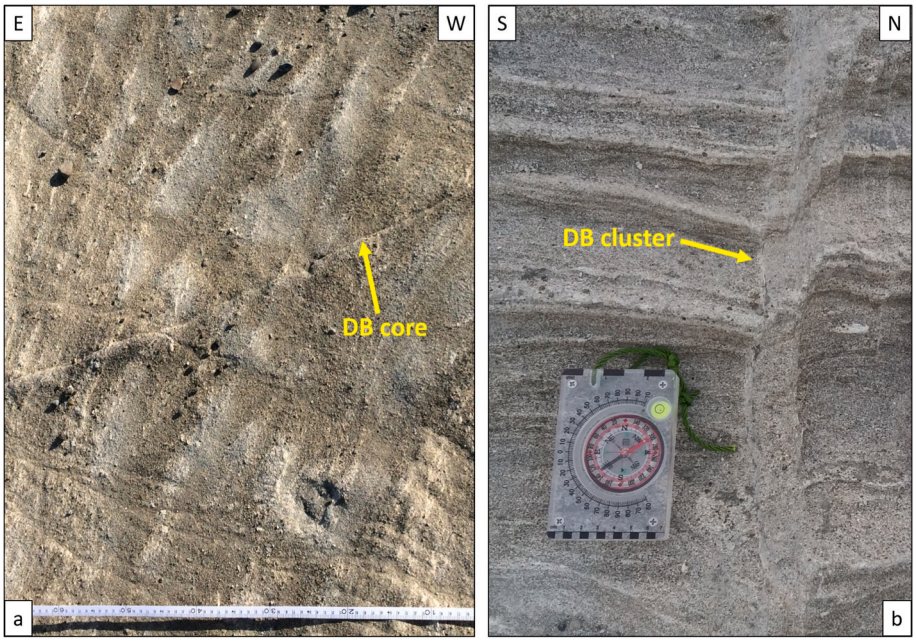

Fig. 9. Field photos of (a) deformation band core and (b) deformation band cluster.

of fine to medium grains in which the average grain size ranged from 0.16 to 0.46 mm. They are usually porous (>5%) with porosities of ~1–~18%, and mean grain crushing pressure ranging from ~47 to ~570 MPa. Most of these tuffs and pyroclastic rocks are poorly-sorted with sorting coefficients larger than 1.0 while few units are moderately well-sorted (Table 1; Fig. 6). The plots of porosity and sorting against grain size (Fig. 7) indicate that these parameters are independent. And the plots reveal a significant variation with the characteristics of lithological units.

4.2. Deformation bands

We classified deformation bands at Shitiping into four kinematic types based on our field investigation. Type 1 bands are pure compaction band with grain disaggregation striking NNE-SSW (Fig. 8a). Type 2 bands are compactional shear bands with reverse shear sense and grain fracturing striking NNE-SSW (Fig. 8b). Type 3 bands, which are most abundant in Shitiping area, are compactional shear bands with strike-slip shear sense with cataclasis (Fig. 3). And Type 4 bands are shear

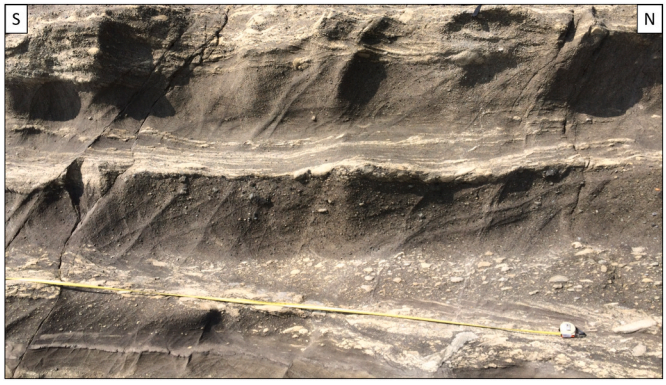

Fig. 10. Field photo demonstrating the variation of deformation band appearances from one lithology to another. The deformation band frequency in tuff (grayish unit) is higher than in tuff with abundant volcanic bombs.

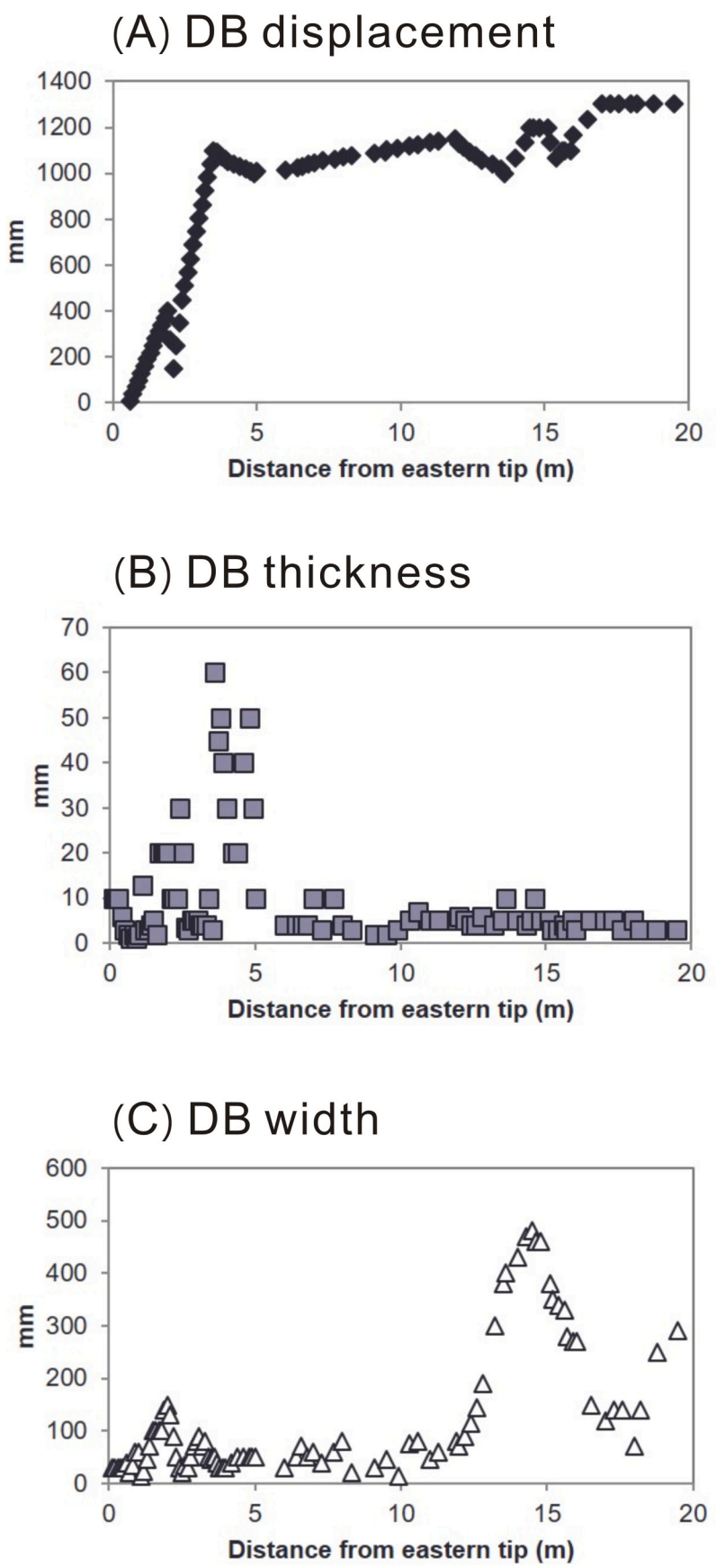

Fig. 11. Variations of maximum cluster displacement (D), core thickness (T) and cluster width (W) of deformation bands documented in Outcrop 1, indicating that displacement magnitude may not be the only control on deformation band core thickness and cluster width.

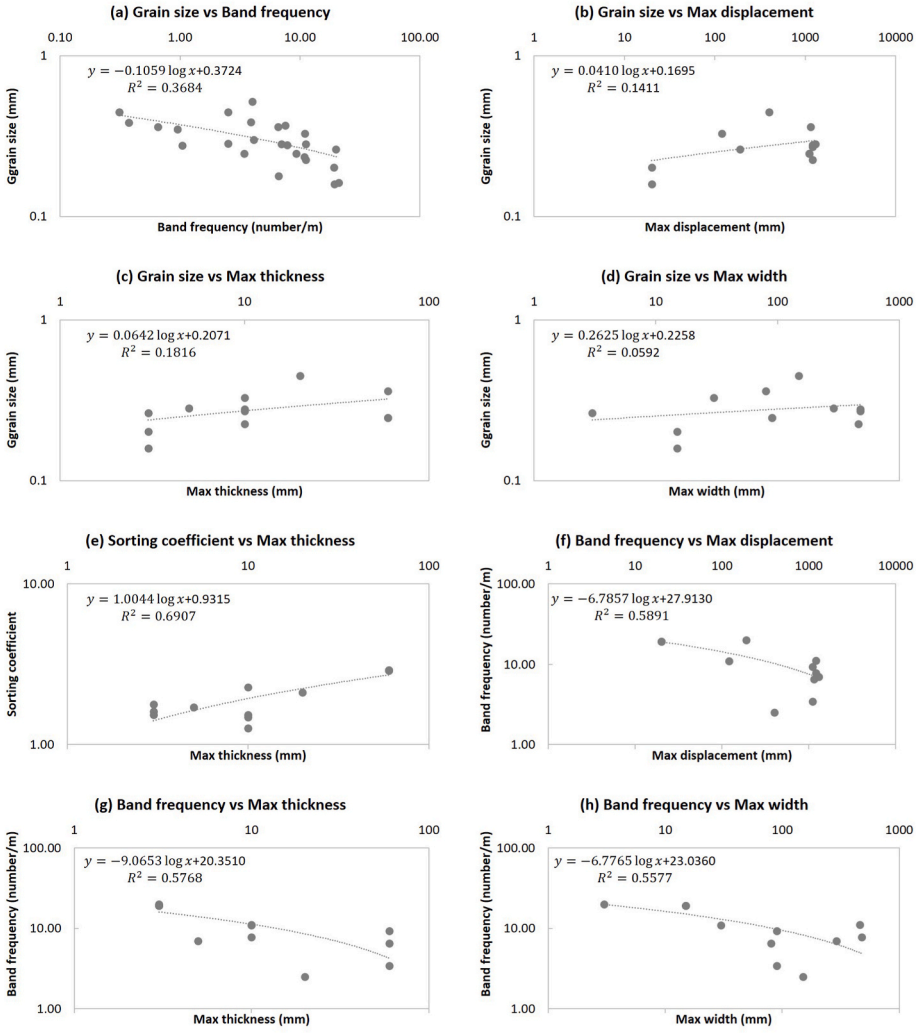

Fig. 12. Correlations between host rock properties and deformation band characteristics. (a) Correlation between average grain size (R) and deformation band frequency (F). (b) Correlation between average grain size (R) and maximum displacement of deformation band (D′). (c) Correlation between average grain size (R) and maximum core thickness of deformation band (T). (d) Correlation between average grain size (R) and maximum cluster width of deformation band (W). (e) Correlation between sorting coefficient (SC) and maximum core thickness of deformation band (D′). (f) Correlation between deformation band frequency (F) and maximum displacement of deformation band (D′). (g) Correlation between deformation band frequency (F) and maximum core thickness of deformation band (T). (h) Correlation between deformation band frequency (F) and maximum cluster width of deformation band (W).

bands with normal shear sense and form along pre-existing Type 3 bands. To explore how lithologic properties influence the occurrence and characteristics of deformation bands, we focus on the well-developed and widely distributed Type 3 bands across a range of host rock lithologies. Type 3 bands that exhibit a dextral shear sense typically strike towards the NE-SW direction, whereas those exhibiting a sinistral shear sense generally strike towards the NW-SE direction (Fig. 8c).

The Type 3 deformation bands exposed at Shitiping may occur as single bands or clustered strands (Fig. 9), and are characterized by highly deformed tabular core zones resulting from pore collapse and grain fracturing with sharp and irregular borders (Figs. 2 and 3). Type 3 deformation bands vary in appearance (band frequency, single or clustered strands) (Figs. 9 and 10) and strain magnitude (intense in cores and conspicuously less in the intervening lenses, Fig. 3), allowing quantitative analysis of deformation band characteristics including the frequency, core thickness of single deformation bands or cluster width of deformation band strands, and displacement of single deformation bands or band clusters.

Deformation band frequency in outcrop 1 ranges from 1.00 to 17.78 bands per meter, with a maximum cluster displacement of 1300 mm and the maximum core thickness and maximum cluster width of 60 mm and 480 mm, respectively. Deformation bands from outcrop 2 have a frequency that ranges from 1.67 to 4.33 bands per meter, with a maximum cluster displacement of 1300 mm, and core thickness and cluster width of 60 mm and 460 mm, respectively. In outcrop 3, the band frequency varies from 1.25 to 66.0 bands per meter.

Our measurement of a deformation band cluster within outcrop 1 has revealed significant lateral variations in the cluster displacement, core thickness, and cluster width (Fig. 11). The locations where maximum cluster width and deformation band core thickness occur does not coincide with the point of maximum shear displacement. In addition, the cluster width varies significantly while shear displacement remains at around 1000–1200 mm. This contradicts the generally accepted concept that band thickness or cluster width increase with increasing displacement, indicating that the amount of displacement is not the main control of deformation band core thickness and cluster width. This observation, along the observed frequency variation of deformation bands between rock units implies that lithological properties of the host rocks may be more important controls on deformation band characteristics.

4.3. Correlations between characteristics of deformation bands and host rock units

To explore the possible roles of lithologic properties on the development of deformation bands, we compared the frequency, maximum core thickness, maximum cluster width and maximum cluster displacement of deformation bands with the porosity, average grain size, sorting coefficient and mean grain crushing pressure of their host rock. In order to minimize effects from site characteristics, we focus on data from Outcrop 1 to clarify the relationships between host rock properties and occurrence of deformation bands.

Correlations using data in Table 1 show that the average grain size

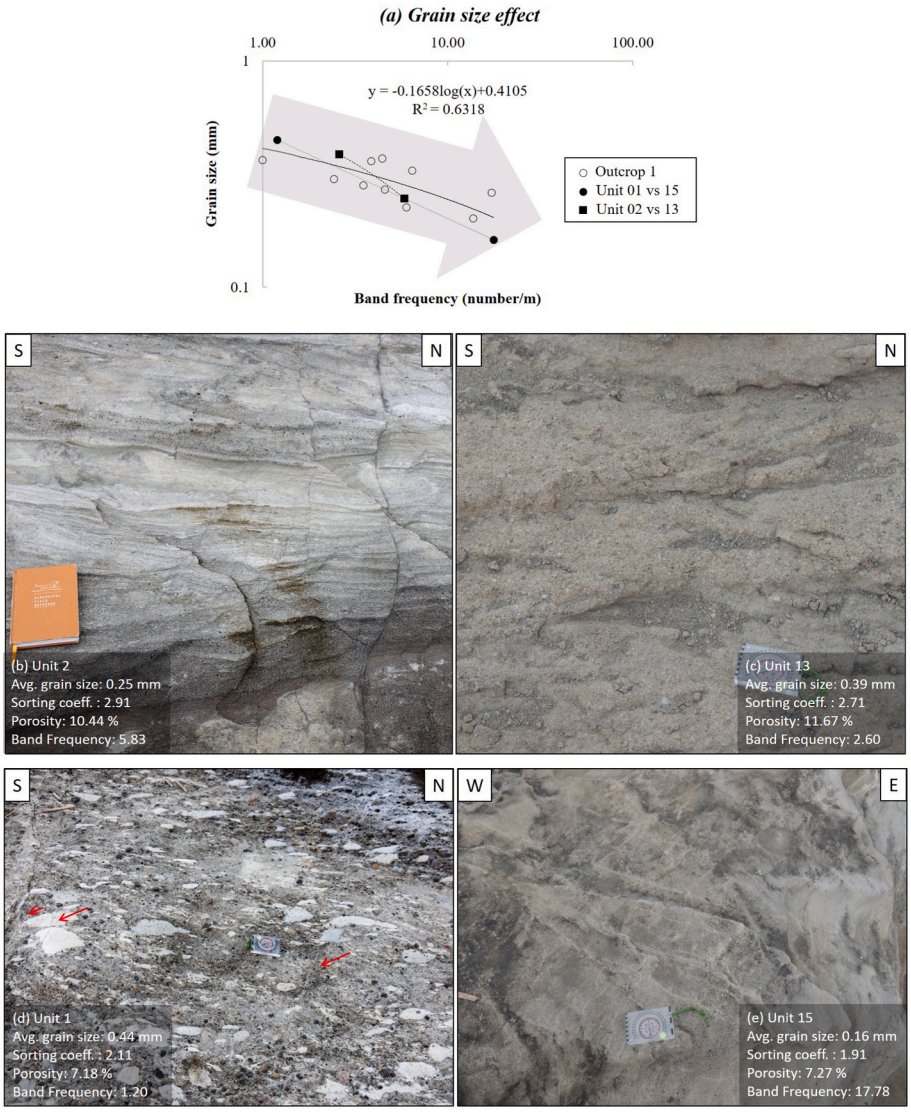

Fig. 13. (a) Grain size effect on occurrence of deformation bands in pyroclastic rocks based on data from Outcrop 1. (b, c) Example of comparison isolating effects from average grain size of host rock: with similar porosity values and sorting coefficients (SC), deformation band frequency is higher in (b) unit of smaller average grain size (unit 2) with respect to (c) unit of larger average grain size (unit 13). (d, e) Example of comparison isolating effects from average grain size of host rock: with similar porosity values and sorting coefficients (SC), deformation band frequency is higher in (e) unit of smaller average grain size (unit 15) with respect to (d) unit of larger average grain size (unit 1).

(R) of pyroclastic rocks at Shitiping is weakly negatively correlated to band frequency and weakly positively related to the maximum cluster displacement, core thickness and cluster width of deformation band (Fig. 12). Band frequency is also found to be negatively correlated to average grain size for pyroclastic rocks in outcrop 1 (Fig. 13). Although there is scatter, the pattern and slope of correlation equation imply that the average grain size might be more dominant in affecting band frequency compared to host rock porosity (Figs. 12 and 13). To isolate the effect of grain size, we also compared layers in Outcrop 1 (unit 1 and unit 15; unit 2 and unit 13) with similar porosity and sorting coefficient but different average grain size (Fig. 13). In all cases, increased average grain size yields lower deformation band frequency (Fig. 13).

The relationships between porosity of pyroclastic rocks and band frequency (F), maximum cluster displacement (D'), core thickness (T) and cluster width (W) of deformation bands exhibit no clear trends, suggesting minimal sensitivity to host rock porosity at Shitiping. There also lacks obvious correlation between porosity and band frequency at outcrop 1 (Fig. 14). To isolate the effect of porosity and band frequency, we show data from two units which vary in porosity but have similar grain size and sorting coefficient (unit 6 and unit 7, Fig. 14). The higher band frequency in unit 7, which is more porous, shows that the porosity might be positively correlated to band frequency (Fig. 14).

Correlations between mean grain crushing pressure (P*) and band frequency, cluster displacement, core thickness and cluster width show no clear trend in our analysis.

The sorting coefficient of host rocks at Shitiping is positively correlated to the maximum core thickness of deformation band (Fig. 12e) but shows no relationship with band frequency. However, isolating rock units with similar grain sizes and porosity values (Unit 2 and 7; Unit 5 and 9; Fig. 15) shows that the sorting coefficient is negatively correlated to band frequency, indicating high deformation band frequency in well-sorted host rocks (Fig. 15).

We also correlated band frequency with maximum core thickness (T), cluster width (W) and cluster displacement (D') for all lithological characterizations and find that band frequency is negatively correlated to the maximum cluster displacement (Fig. 12f), core thickness (Fig. 12g) and cluster width (Fig. 12h).

5. Discussions - implications for lithological effects on deformation band development

Compared to published lithological effect models for well-sorted sandstones (e.g. Soliva et al., 2013), our data show more scatter, likely due to varied grain composition and rapid lateral facies changes of tuffs and pyroclastic rocks. However, the Shitiping deformation bands that developed under similar stress regime still exhibit patterns indicating

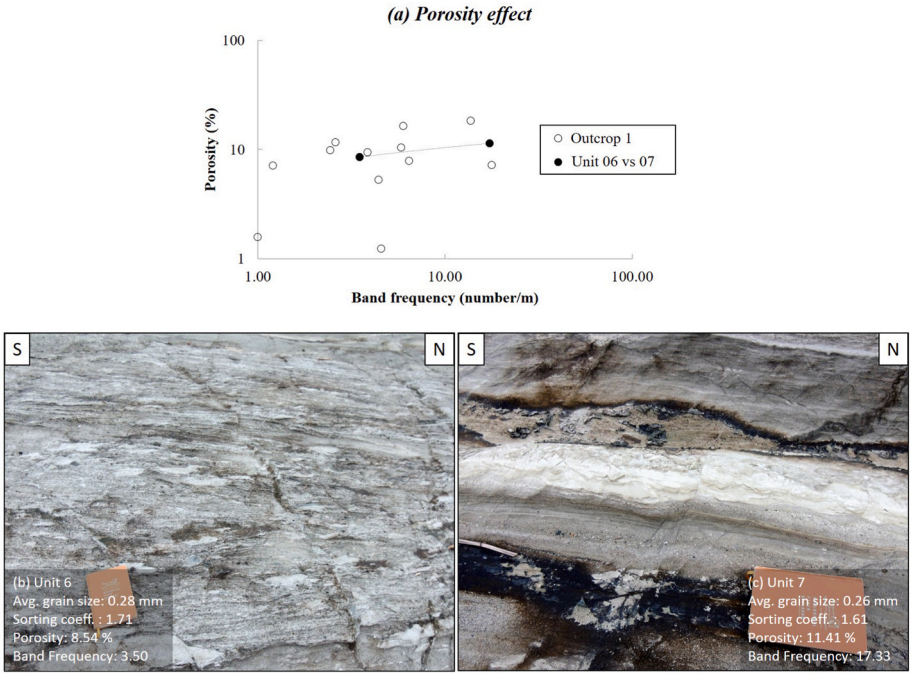

Fig. 14. (a) Porosity effect on occurrence of deformation bands in pyroclastic rocks based on data from Outcrop 1. (b, c) Example of comparison isolating host rock porosity effects: with similar average grain sizes and sorting coefficients (SC), deformation band frequency is higher in (c) unit of higher porosity (unit 7) with respect to (b) unit of lower porosity (unit 6).

possible host rock – deformation band relationships.

Deformation bands in pyroclastic rocks result from grain crushing and pore collapse which lead to reduced grain size and lowered porosity. In pyroclastic rocks, alteration and mineralization in deformation bands are also common (Wilson et al., 2003) and affect associated lithological properties and deformation band occurrences such as band frequency, core thickness and cluster width. Therefore, site characteristics may also play a role and complicate the factor analysis. For the studied Shitiping locality, the three outcrops are separated by faults and thus each outcrop might have accumulated different amount of strain. Additionally, the characteristics of host rocks in each outcrop vary, adding to scatter in our data.

5.1. Porosity effect

Porosity plays an important role in rock failure and strength (Baud et al., 2014; Wong and Baud, 2012; Zhang et al., 1990), for example uniaxial compressive strength being inversely proportional to rock porosity (Zhu et al., 2011). Porosity has also been shown to affect the distribution and type of deformation bands in quartz-rich sandstone, tuffs and pyroclastic rock (Schultz et al., 2010; Cavailhes and Rotevatn, 2018). The clearest example of how porosity can influence deformation band development is the existence of pure compaction bands in layers with highest porosity and largest grain size in Jurassic Navajo sandstone (Schultz et al., 2010).

Our observations of deformation bands in pyroclastic rocks at the Shitiping area show that the band frequency is higher in units with higher porosity (Fig. 16). Such results are similar to the trend found in sandstone reported by Soliva et al. (2013). Rock mechanics experiments and thin section observations of Alban Hills Tuff by Zhu et al. (2011) also indicated that the inelastic compaction behavior of samples is primarily associated with pore collapse. Wong and Baud (2012) pointed out that the initial strain in ignimbrite and carbonate rocks concentrates around pore space, indicating that pore collapse is one of the main processes of contractional deformation in porous material based on thin section observations. Numerical models of ductile deformation in porous material led to the same conclusion showing regions with higher porosity promoting plastic flow localization into a deformation band (Becker, 1987). These works demonstrated that the strain mainly accumulates in regions with higher porosity where inhomogeneous materials deformed due to pore collapse, thus deformation bands tend to develop in tuff and pyroclastic rock units with high porosity.

Numerical models of Chemenda et al. (2014) indicated that the spacing of deformation bands is controlled by the stiffness contrast between layers. The model showed that the spacing of deformation band decreases where the stiffness of bounding layers increases. Since the stiffness is negatively proportional to porosity (Hardin and Beckermann, 2007), highly porous rocks are more prone to develop deformation bands with high frequency.

5.2. Grain size effect

Our observations of deformation bands in pyroclastic rocks at the Shitiping area show that the band frequency is higher in units with smaller average grain size (Fig. 16). We postulate that this is due to the effect of grain contact density on degree of strain localization. As grain size increases, the contacts per unit volume decrease accordingly. This decrease in grain contacts promotes stress concentration and results in high value of compressive stress on grain contacts, leading to fracturing of grains (Antonellini et al., 1994). Numerical experiments also supported the concept of grain size effect. The relative sizes between elements and sample in the numerical experiments can cause different value of contact forces. In general, larger element size results in larger contact forces (Antonellini and Aydin, 1994), resulting in fracturing of grains. This fracturing of large grains is key to initiation of deformation band development. We infer that the low grain contact density inhibits the formation of more deformation bands and leads to lower deformation band frequency.

In contrast, the trend we identify is different from the trend published by Soliva et al. (2013), Griffiths et al. (2016) and Skurtveit et al. (2014). Based on data gathered from the Uchaux and Orange sandstones, Soliva et al. (2013) published a summary model showing that the frequency of deformation bands was positively correlated to host rock grain size. However, the grain size range in Soliva et al. (2013) was

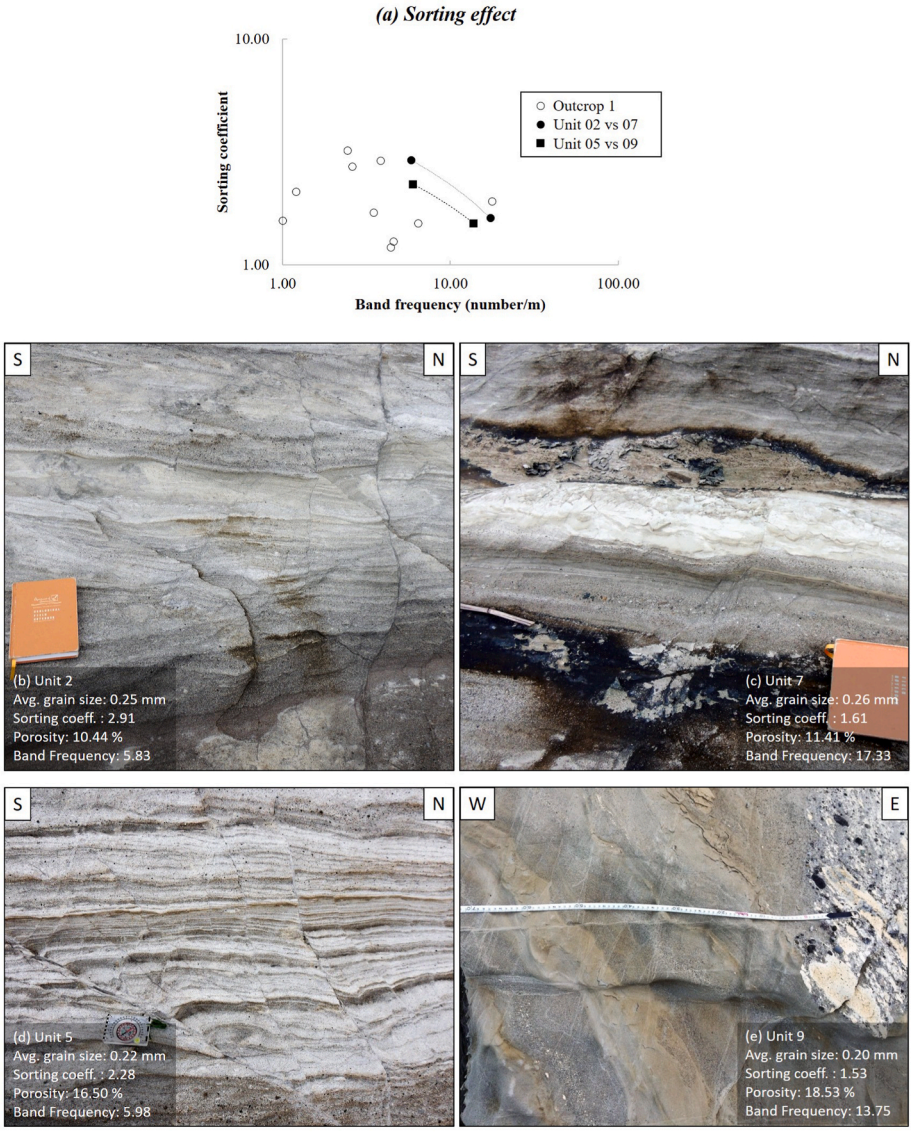

Fig. 15. (a) Sorting effect on occurrence of deformation bands in pyroclastic rocks based on data from Outcrop 1. (b, c) Example of comparison isolating effects from sorting coefficient (SC) of host rock: with similar porosity values and average grain sizes, deformation band frequency is higher in (c) well-sorted unit of lower SC (unit 7) with respect to (b) poorly sorted unit (unit 2). (d, e) Example of comparison isolating effects from sorting coefficient (SC) of host rock: with similar porosity values and average grain sizes, deformation band frequency is higher in (e) well-sorted unit of lower SC (unit 9) with respect to (d) poorly sorted unit (unit 5).

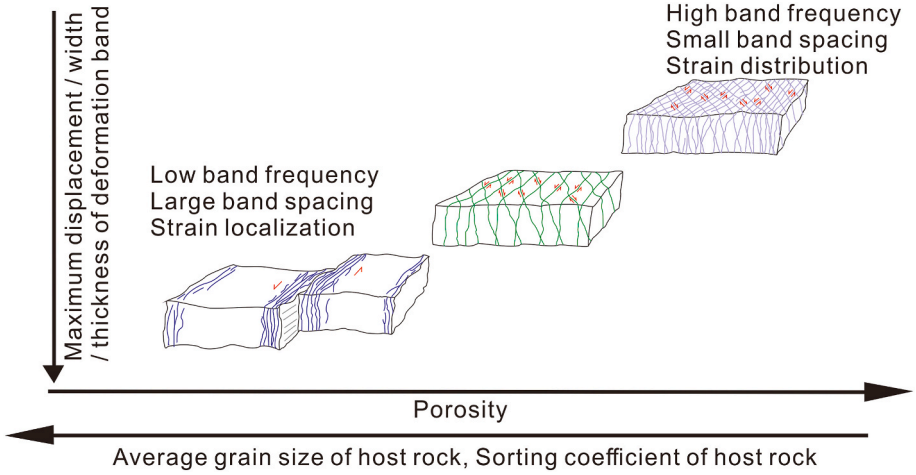

Fig. 16. Lithological effects on occurrence of deformation bands in pyroclastic rocks based on data from Outcrop 1. Porosity of host rocks are positively correlated to frequency (F) of deformation band, whereas average grain size and sorting coefficient are negatively correlated. Maximum displacement, thickness and width of band are also weakly correlated to the above host rock properties.

0.74–1.18 mm, while ours is 0.16–0.45 mm. This might imply scale effects of grain size ranges or lithology/mineral composition on deformation band frequency. Griffiths et al. (2016) studied how the intrinsically variable characteristics of sandstones influenced the distribution of deformation bands in Triassic Sherwood Sandstone at Thurstaston, UK, and found that deformation bands were predominantly restricted to poorly sorted and coarse-grained sandstones. Research in Boncavaï quarry (Bassin du Sud-Est, Provence, France) made by Skurtveit et al. (2014) suggested that the preferential localization of SECB in coarse-grained sandstone was controlled by: (1) higher stress concentration on grain contact; and (2) faster compaction and slightly denser packing during band formation. The disparity between published results and those documented in the Shitiping pyroclastics may be mainly due to differences in mineralogical composition and sorting of the host rock. Preferred fracturing of weaker grains such as feldspar or volcanic glass in host rock has been observed (Cavailhes and Rotevatn, 2018; Del Sole and Antonellini, 2019). Del Sole et al., (2020) mentioned the preferred fracturing of feldspar grains instead of quartz grains, and the different fracturing mechanism (intragranular fracturing of feldspar; spalling and flanking of edges of quartz) in arkose sandstone. The preferred fracturing can affect the mechanical properties and thus influence stress and strain distribution, which potentially plays a role in causing different grain size effects on deformation band frequency. Different grain size effects on band frequency between pyroclastic rocks and quartz-rich sandstones imply that mineralogical composition might also be important in affecting the development of deformation bands.

5.3. Sorting coefficient effect

Our observations of deformation bands in pyroclastic rocks at the Shitiping area show that the band frequency is higher in units with higher sorting coefficient (Fig. 16). This phenomenon agrees with findings in quartz sandstones, as deformation bands (pure compaction bands) occur in layers with narrow grain size ranges for Aztec and Navajo sandstones (Antonellini et al., 2014; Cheung et al., 2012; Eichhubl et al., 2010; Mollema and Antonellini, 1996; Schultz et al., 2010). Compression tests on both well- and poorly-sorted Boise sandstone over a wide range of pressure produced compaction localization as compaction bands only in well-sorted samples (Cheung et al., 2012), demonstrating that compaction localization is controlled by grain size distribution and is more prone to occur in well-sorted rocks.

The mechanism behind sorting effect on deformation band development may be related to grain reduction processes and strain distribution. Griffiths et al. (2016) suggested that non-uniform grain-size distribution allows smaller grains to distribute the load over large particles, hence reducing stress concentration between the grains and inhibiting deformation band development in poorly sorted sandstone. Based on undisturbed fault gouge samples from the Lopez fault zone in the San Gabriel Mountains, Sammis et al. (1987) proposed that the failure probability of grains depends on the relative size of nearest neighbors and the fractal dimension of particle. Numerical experiments of Antonellini and Aydin (1994) are in agreement with the idea of Sammis et al. (1987) and Griffiths et al. (2016). Results of DEM experiments revealed that grain size distribution can affect the required stress during deformation, and that unsorted distribution of grain size material requires greater stresses to deform (Antonellini and Aydin, 1994). 3D numerical simulation results of Abe and Mair (2005) found that high grain comminution rate and fast destruction of large clasts occur mainly during initial strain accumulation. These results imply that the small grains around large grains may play an important role in keeping large grains intact and preventing strain localization structures from developing in poorly-sorted rocks, which might be the reason for the positive correlation between sorting and deformation band frequency.

6. Conclusion

The spectacular exposures of deformation bands in pyroclastic rocks at Shitiping, eastern Taiwan are quantitatively analyzed to explore lithological effects on deformation band development. Clear definition and description of quantitative deformation band characteristics including deformation band frequency, deformation band core thickness, deformation band cluster width, deformation band core displacement and deformation band cluster displacement are proposed in a classification scheme based on detailed field observations, and are demonstrated in field measurements. Host rock properties including porosity, average grain size, sorting coefficient and derived mean grain crushing pressure are acquired from thin section analyses and correlated with the deformation band characteristics. The correlation reveals that the deformation band frequency tends to be higher in tuff and pyroclastic rocks with smaller average grain size, higher porosity, better sorting and higher mean grain crushing pressure. Core thickness is observed to be related to average grain size and sorting of host rock. Correlation also shows that cluster width of deformation bands is affected by average grain size. The relations among frequency of deformation bands with porosity and sorting of host rock in the Shitiping pyroclastics are similar in trend with those found in well-sorted quartz sandstones. Correlations between average grain size of pyroclastic rocks and deformation band frequency are different from the relation revealed by quartz-rich sandstone. We postulate the discrepancy might be due to differences in mineral compositions and grain size ranges. Our findings indicate that the host rock properties influence the occurrences of deformation bands. Development and architecture of deformation bands in pyroclastic rocks can therefore be estimated or forecasted based on host rock properties.

Author statement

Chih-Cheng Chung: Investigation, Methodology, Formal analysis, Writing-original draft, Revision, Visualization.

Chih-Tung Chen: Writing-review & editing, Revision, Methodology, Resources, Supervision, Funding acquisition.

Chia-Yu Lu: Conceptualization, Methodology, Resources, Supervision.

Declaration of competing interest

The authors declare that they have no known competing financial interests or personal relationships that could have appeared to influence the work reported in this paper.

Data availability

Data will be made available on request.

Acknowledgements

We are grateful to the constructive and detailed comments from Marco Antonellini and anonymous Reviewers as well as Editor Fabrizio Agosta. We sincerely acknowledge Jian-Cheng Lee, Yu-Chang Chan, Hao-Tsu Chu, Fu-Shu Jeng, En-Chao Yeh, Kuo-Jen Chang, Roman DiBiase, Thibault Cavailhes and Atle Rotevatn for their insightful advises and discussions. Kuo-Jen Chang kindly constructed the DSM, Shih-Wei Wang and Kun-Wei Chung helped producing polished thin sections. This work is financially supported by grants (110-2116-M-008-008- and 111-2116-M-008-019- to CTC) from National Science and Technology Council, Taiwan, R.O.C. and National Central University grants to CTC.

References

Abe, S., Mair, K., 2005. Grain fracture in 3D numerical simulations of granular shear. Geophys. Res. Lett. 32, L05305 https://doi.org/10.1029/2004GL022123.

Antonellini, M., Aydin, A., 1994. Effect of faulting on fluid flow in porous sandstones: petrophysical properties. AAPG Bull. 78 (3), 355–377.

Antonellini, M.A., Aydin, A., Pollard, D.D., 1994. Microstructure of deformation bands in porous sandstones at Arches National Park, Utah. J. Struct. Geol. 16 (7), 941–959.

Antonellini, M., Petracchini, L., Billi, A., Scrocca, D., 2014. First reported occurrence of deformation bands in a platform limestone, the Jurassic Calcare Massiccio Fm., northern Apennines, Italy. Tectonophysics 628, 85–104.

Ballas, G., Soliva, R., Sizun, J.-P., Benedicto, A., Cavailhes, T., Raynaud, S., 2012. The importance of the degree of cataclasis in shear bands for fluid flow in porous sandstone, Provence, France. AAPG (Am. Assoc. Pet. Geol.) Bull. 96 (11), 2167–2186.

Ballas, G., Fossen, H., Soliva, R., 2015. Factors controlling permeability of cataclastic deformation bands and faults in porous sandstone reservoirs. J. Struct. Geol. 76, 1–21.

Ballas, G., Soliva, R., Benedicto, A., Sizun, J.-P., 2014. Control of tectonic setting and large-scale faults on the basin-scale distribution of deformation bands in porous sandstone (Provence, France). Mar. Petrol. Geol. 55, 142–159.

Baud, P., Wong, T.-F., Zhu, W., 2014. Effects of porosity and crack density on the compressive strength of rocks. Int. J. Rock Mech. Min. Sci. 67, 202–211.

Becker, R., 1987. The effect of porosity distribution on ductile failure. J. Mech. Phys. Solid. 35 (5), 577–599.

Cashman, S., Cashman, K., 2000. Cataclasis and deformation-band formation in unconsolidated marine terrace sand, Humboldt County, California. Geology 28 (2), 111–114.

Cavailhes, T., Rotevatn, A., 2018. Deformation bands in volcaniclastic rocks - insights from the shihtiping tuffs, coastal range of taiwan. J. Struct. Geol. 113, 155–175.

Chemenda, A.I., Ballas, G., Soliva, R., 2014. Impact of a multilayer structure on initiation and evolution of strain localization in porous rocks: field observations and numerical modeling. Tectonophysics 631, 29–36.

Cheung, C.S.N., Baud, P., Wong, T.-F., 2012. Effect of grain size distribution on the development of compaction localization in porous sandstone. Geophys. Res. Lett. 39, L21302 https://doi.org/10.1029/2012GL053739.

Clifton, A.E., Kattenhorn, S.A., 2006. Structural architecture of a highly oblique divergent plate boundary segment. Tectonophysics 419, 27–40.

Davatzes, N.C., Aydin, A., Eichhubl, P., 2003. Overprinting faulting mechanisms during the development of multiple fault sets in sandstone, Chimney Rock fault array, Utah, USA. Tectonophysics 363, 1–18.

Del Sole, L., Antonellini, M., 2019. Microstructural, petrophysical, and mechanical properties of compactive shear bands associated to calcite cement concretions in arkose sandstone. J. Struct. Geol. 126, 51–68.

Del Sole, L., Antonellini, M., Soliva, R., Ballas, G., Balsamo, F., Viola, G., 2020. Structural control on fluid flow and shallow diagenesis: insights from calcite cementation along deformation bands in porous sandstones. Solid Earth 11 (6), 2169–2195.

Eichhubl, P., Hooker, J.N., Laubach, S.E., 2010. Pure and shear-enhanced compaction bands in Aztec Sandstone. J. Struct. Geol. 32 (12), 1873–1886.

Folk, R.L., Ward, W.C., 1957. Brazos River bar: a study in the significance of grain size parameters. J. Sediment. Res. 27 (1), 3–26.

Fossen, H., Schultz, R.A., Shipton, Z.K., Mair, K., 2007. Deformation bands in sandstone: a review. J. Geol. Soc. 164 (4), 755–769.

Fossen, H., Soliva, R., Ballas, G., Trzaskos, B., Cavalcante, C., Schultz, R.A., 2018. A review of deformation bands in reservoir sandstones: geometries, mechanisms and distribution. Geological Society, London, Special Publications 459 (1), 9–33.

Gillespie, M., Styles, M., 1999. BGS Rock Classification Scheme, Volume 1. Classification of Igneous Rocks. British Geological Survey Research Report, (2nd Edition), p. 52.

Griffiths, J., Faulkner, D.R., Edwards, A.P., Worden, R.H., 2016. Deformation band development as a function of intrinsic host-rock properties in Triassic Sherwood Sandstone. Geological Society, London, Special Publications 435 (1), 161–176.

Hardin, R.A., Beckermann, C., 2007. Effect of porosity on the stiffness of cast steel. Metall. Mater. Trans. 38 (12), 2992–3006.

Hesthammer, J., Fossen, H., 2000. Uncertainties associated with fault sealing analysis. Petrol. Geosci. 6 (1), 37–45.

Huang, C.-Y., Yuan, P.B., Teng, L.S., 1988. Paleontology of the kangkou limestone in the middle coastal range, eastern taiwan. Acta Geol. Taiwan. 26, 133–160.

Kaproth, B.M., Cashman, S.M., Marone, C., 2010. Deformation band formation and strength evolution in unlithified sand: the role of grain breakage. J. Geophys. Res. Solid Earth 115, B12103. https://doi.org/10.1029/2010JB007406.

Kong, M., Bhattacharya, R.N., James, C., Basu, A., 2005. A statistical approach to estimate the 3D size distribution of spheres from 2D size distributions. Geol. Soc. Am. Bull. 117 (1–2), 244–249.

Lai, W.-J., 1995. A Study on the Characteristics of the Structures in the Middle Part of Coastal Range, Eastern Taiwan. National Cheng Kung University, p. 122.

Lai, Y.-M., Song, S.-R., Lo, C.-H., Lin, T.-H., Chu, M.-F., Chung, S.-L., 2017. Age, geochemical and isotopic variations in volcanic rocks from the coastal range of taiwan: implications for magma generation in the northern Luzon Arc. Lithos 272, 92–115.

Lin, S.-T., Huang, W.-J., 2017. Deformation Bands in Shihtiping, Eastern Taiwan, vol. 31. Special Publication of the Central Geological Survey, pp. 35–64.

Lu, C.-Y., Hsu, K.J., 1992. Tectonic evolution of the Taiwan mountain belt. Petrol. Geol. Taiwan 29, 15–35.

Mollema, P.N., Antonellini, M.A., 1996. Compaction bands: a structural analog for anti-mode I cracks in aeolian sandstone. Tectonophysics 267, 209–228.

Philit, S., Soliva, R., Castilla, R., Ballas, G., Taillefer, A., 2018. Clusters of cataclastic deformation bands in porous sandstones. J. Struct. Geol. 114, 235–250.

Riley, P.R., Goodwin, L.B., Lewis, C.J., 2010. Controls on fault damage zone width, structure, and symmetry in the Bandelier Tuff, New Mexico. J. Struct. Geol. 32 (6), 766–780.

Rotevatn, A., Thorsheim, E., Bastesen, E., Fossmark, H.S., Torabi, A., Sælen, G., 2016. Sequential growth of deformation bands in carbonate grainstones in the hangingwall of an active growth fault: implications for deformation mechanisms in different tectonic regimes. J. Struct. Geol. 90, 27–47.

Rotevatn, A., Torabi, A., Fossen, H., Braathen, A., 2008. Slipped deformation bands: a new type of cataclastic deformation bands in Western Sinai, Suez rift, Egypt. J. Struct. Geol. 30 (11), 1317–1331.

Rotevatn, A., Tveranger, J., Howell, J.A., Fossen, H., 2009. Dynamic investigation of the effect of a relay ramp on simulated fluid flow: geocellular modelling of the Delicate Arch Ramp, Utah. Petrol. Geosci. 15 (1), 45–58.

Rustichelli, A., Tondi, E., Agosta, F., Cilona, A., Giorgioni, M., 2012. Development and distribution of bed-parallel compaction bands and pressure solution seams in carbonates (Bolognano Formation, Majella Mountain, Italy). J. Struct. Geol. 37, 181–199.

Sammis, C., King, G., Biegel, R., 1987. The kinematics of gouge deformation. Pure Appl. Geophys. 125 (5), 777–812.

Schultz, R., Siddharthan, R., 2005. A general framework for the occurrence and faulting of deformation bands in porous granular rocks. Tectonophysics 411 (1), 1–18.

Schultz, R.A., Okubo, C.H., Fossen, H., 2010. Porosity and grain size controls on compaction band formation in Jurassic Navajo Sandstone. Geophys. Res. Lett. 37, L22306 https://doi.org/10.1029/2010GL044909.

Shipton, Z., Evans, J., Thompson, L., 2005. The geometry and thickness of deformation-band fault core and its influence on sealing characteristics of deformation-band fault zones. AAPG Memoir 85, 181–195.

Skurtveit, E., Ballas, G., Fossen, H., Torabi, A., Soliva, R., Peyret, M., 2014. Sand textural control on shear-enhanced compaction band development in poorly-lithified sandstone. J. Geol. Resour. Eng. 2, 115–130.

Soliva, R., Ballas, G., Fossen, H., Philit, S., 2016. Tectonic regime controls clustering of deformation bands in porous sandstone. Geology 44 (6), 423–426.

Soliva, R., Schultz, R.A., Ballas, G., Taboada, A., Wibberley, C., Saillet, E., Benedicto, A., 2013. A model of strain localization in porous sandstone as a function of tectonic setting, burial and material properties; new insight from Provence (southern France). J. Struct. Geol. 49, 50–63.

Song, S.-R., 1990. A Study of the Volcanic Rocks in the Central Coastal Range of Eastern Taiwan and the Evolution of Volcanic Island Arc of the Northern Luzon Arc. Ph. D. dissertation. Institute of Geology, National Taiwan University, p. 251.

Song, S.-R., Lo, H.-J., 1987. Volcanic rocks of the coastal range of Taiwan as the products of submarine eruption: the evidence from Loho area. Acta Geol. Taiwan. 25, 97–109.

Song, S.-R., Lo, H.-J., 2002. Lithofacies of volcanic rocks in the central Coastal Range, eastern Taiwan: implications for island arc evolution. J. Asian Earth Sci. 21 (1), 23–38.

Teng, L.S., 1990. Geotectonic evolution of late Cenozoic arc-continent collision in Taiwan. Tectonophysics 183 (1–4), 57–76.

Wilson, J.E., Goodwin, L.B., Lewis, C.J., 2003. Deformation bands in nonwelded ignimbrites: petrophysical controls on fault-zone deformation and evidence of preferential fluid flow. Geology 31 (10), 837–840.

Wilson, J.E., Goodwin, L.B., Lewis, C., 2006. Diagenesis of deformation band faults: record and mechanical consequences of vadose zone flow and transport in the Bandelier Tuff, Los Alamos, New Mexico. J. Geophys. Res. Solid Earth 111, B09201. https://doi.org/10.1029/2005JB003892.

Wong, T.-F., Baud, P., 2012. The brittle-ductile transition in porous rock: a review. J. Struct. Geol. 44, 25–53.

Zhang, J., Wong, T.-F., Davis, D.M., 1990. Micromechanics of pressure-induced grain crushing in porous rocks. J. Geophys. Res. 95 (B1), 341–352. https://doi.org/10.1029/JB095iB01p00341.

Zhu, W., Baud, P., Vinciguerra, S., Wong, T.F., 2011. Micromechanics of brittle faulting and cataclastic flow in Alban Hills tuff. J. Geophys. Res. Solid Earth 116, B06209. https://doi.org/10.1029/2010JB008046.